

Dynamics of silicon metabolism and silicon isotopic discrimination in a marine diatom as a function of $p\text{CO}_2$

Allen J. Milligan¹

Department of Geosciences, Princeton University, Princeton, New Jersey 08544

Diana E. Varela² and Mark A. Brzezinski

Department of Ecology, Evolution, and Marine Biology and the Marine Science Institute, University of California, Santa Barbara, California 93106

François M. M. Morel

Department of Geosciences, Princeton University, Princeton, New Jersey 08544

Abstract

Opal accumulation rates in sediments have been used as a proxy for carbon flux, but there is poor understanding of the factors that regulate the Si quota of diatoms. Natural variation in silicon isotopes ($\delta^{30}\text{Si}$) in diatom frustules recovered from sediment cores are an alternative to opal mass for reconstructing diatom Si use and potential C export over geological timescales. Understanding the physiological factors that may influence the Si quota and the $\delta^{30}\text{Si}$ isotopic signal is vital for interpreting biogenic silica as a paleoproxy. We investigated the influence of $p\text{CO}_2$ on the Si quota, fluxes across the cell membrane, and frustule dissolution in the marine diatom *Thalassiosira weissflogii* and determined the effect that $p\text{CO}_2$ has on the isotopic fractionation of Si. We found that our Si flux estimates mass balance and, for the first time, describe the Si budget of a diatom. The Si quota rose in cells grown with low $p\text{CO}_2$ (100 ppm) compared with controls (370 ppm), and the increased quota was the result of greater retention of Si (i.e., lower losses of Si through efflux and dissolution). The ratio of efflux : influx decreased twofold as $p\text{CO}_2$ decreased from 750 to 100 ppm. The efflux of silicon is shown to significantly bias measurements of silica dissolution rates determined by isotope dilution, but no effect on the Si isotopic enrichment factor (ϵ) was observed. The latter effect suggests that silicon isotopic discrimination in diatoms is set by the Si transport step rather than by the polymerization step. This observation supports the use of the $\delta^{30}\text{Si}$ signal of biogenic silica as an indicator of the percentage utilization of silicic acid.

Diatoms play an important role in the export of carbon to the deep sea and control the reverse weathering of silicon in the oceans. This is caused by their high productivity and absolute requirement for silicon in cell wall formation. Silica production has been hypothesized to be a useful proxy of current and past carbon export production (Dugdale and Wilkerson 1998; Ragueneau et al. 2000). The usefulness of this proxy is dependent on understanding the factors that influence the Si : C ratio of the phytoplankton community as

a whole and diatoms in particular, as well as the dissolution of silica during sinking and the preservation efficiency of silica in sediments.

Here we focus on cellular level processes and investigate the effects of growth conditions on silicic acid ($\text{Si}(\text{OH})_4$) metabolism in the marine diatom *Thalassiosira weissflogii* under saturating concentrations ($[\text{Si}(\text{OH})_4] \geq 40 \mu\text{mol L}^{-1}$) of silicic acid. A number of studies have measured the fluxes of Si in diatoms, but none have measured all fluxes under the same conditions (e.g., Sullivan 1976; Ragueneau et al. 2001 and references therein).

There are four important cellular fluxes of $\text{Si}(\text{OH})_4$ (if we ignore the fluxes between intracellular compartments) (Fig. 1): (1) Influx is the transport rate across the plasmalemma from outside to inside the cell. (2) Incorporation is the rate of frustule formation (simply calculated as Si cell^{-1} multiplied by the specific growth rate μ^{-d}). (3) Efflux is the outward transport rate across the plasmalemma, either via the Si transporter or diffusion of some Si species (the internal speciation of Si is not known). (4) Dissolution is the rate of depolymerization of silica to silicic acid. We can also calculate two additional fluxes. (5) Loss is the sum of dissolution and efflux. (6) Net uptake is the difference between influx and loss.

Silicic acid efflux has, to date, not been measured under steady-state silicic acid concentrations in diatoms, but work under non-steady-state conditions has shown that efflux is

¹ Present address: Institute of Marine and Coastal Sciences, Rutgers University, 71 Dudley Road, New Brunswick, New Jersey 08901 (allenm@princeton.edu).

² Present address: Department of Biology & School of Earth and Ocean Sciences University of Victoria, Victoria, British Columbia V8W 3N5, Canada.

Acknowledgments

We thank Michael Bender and Danny Sigman for helpful discussions. Phillippe Tortell provided advice and materials for the silicon oil centrifugation method. Janice Jones helped in running samples for silicon isotopic ratios in the mass spectrometer. Two anonymous reviewers provided comments on the manuscript.

Funding was provided by Center for Bioinorganic Chemistry NSF/CEBIC grant CHE 0221978, National Science Foundation (NSF) Biocomplexity grant DEB-0083566 to A.J.M. and F.M.M.M., NSF grant OCE-9729996 to M.A.B., and an NSERC postdoctoral fellowship to D.E.V.

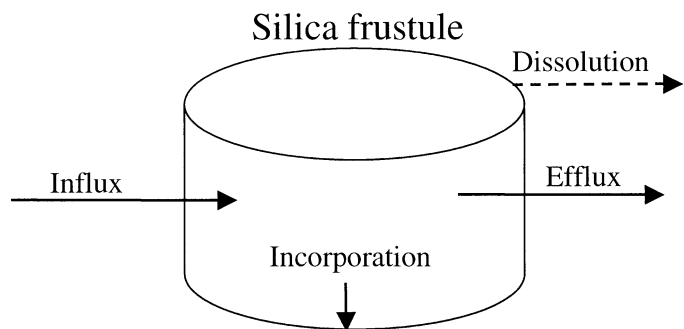


Fig. 1. Diatom silicon fluxes. Influx: the transport rate across the plasmalemma from outside to inside the cell, incorporation: the rate of frustule formation ($\text{Si cell}^{-1} \times \mu^{-d}$), efflux: the transport rate across the plasmalemma from inside to outside the cell, dissolution: the rate of depolymerization of silica to $\text{Si}(\text{OH})_4$. Loss = dissolution + efflux. Net uptake = influx - loss.

positively correlated to the external concentration of $\text{Si}(\text{OH})_4$ (Sullivan 1976). Nutrient effluxes under steady-state conditions are commonly measured in vascular plants (MacRobbie 1971; Britto and Kronzucker 2001), and we applied those techniques to measuring the $\text{Si}(\text{OH})_4$ effluxes in diatoms.

Diatoms fractionate isotopes of silicon, discriminating against the heavier (^{30}Si) isotope (De La Rocha et al. 1997). Natural variations in isotopes of biogenic silica from sediment cores can potentially be used to estimate the relative utilization of Si in surface waters over geological timescales (De La Rocha et al. 1998; Brzezinski et al. 2002). Understanding the physiological factors that may influence the Si isotopic signal is vital for interpreting the $\delta^{30}\text{Si}$ of biogenic silica. The $\delta^{30}\text{Si}$ signal in diatoms has been shown to be unaffected by growth temperature and dissolution of the frustule (De La Rocha et al. 1998), but the physiological mechanism that leads to fractionation is not known. Specifically, it is unknown whether fractionation occurs during Si transport across the cell membrane or during silica deposition. The influence of changes in the ratio of $\text{Si}(\text{OH})_4$ influx to $\text{Si}(\text{OH})_4$ efflux on the silica $\delta^{30}\text{Si}$ can provide insight as to the mechanism of fractionation. By analogy to stable carbon isotopes and given the assumption of an intracellular isotopic discrimination step, we expect that fractionation would be maximal at a high efflux:influx ratio, because a high efflux rate decreases the likelihood that the heavy isotope (^{30}Si) will be incorporated into silica before it is lost from the cell. A low efflux:influx ratio increases the likelihood that the heavy isotope will react within the cell and become incorporated into the frustule, resulting in diminished fractionation. The overall isotope effect is related to the flux ratio according to the equation

$$\varepsilon_f = \varepsilon_{i_1} + (\varepsilon_p - \varepsilon_{i_2})\rho_e/\rho_i \quad (1)$$

where ε_f is the isotope effect measured in the frustule, ε_{i_1} is the isotope effect for transport into the cell, ε_{i_2} is the isotope effect for transport out of the cell, ε_p is the isotope effect for polymerization, and ρ_e/ρ_i is the efflux:influx ratio (Popp et al. 1989). Hence, the overall isotope effect is a linear function of the flux ratio.

Recent evidence that the siliceous cell wall of diatoms is

an effective pH buffer for the enzyme carbonic anhydrase and that it enables the enzymatic conversion of bicarbonate to CO_2 suggests that the silicon metabolism may be influenced by the partial pressure of CO_2 ($p\text{CO}_2$) (Milligan and Morel 2002). Here we investigate the influence of an environmentally realistic range of $p\text{CO}_2$ (0.3–2 times atmospheric $p\text{CO}_2$) on the Si quota and fluxes across the cell membrane in asynchronous cultures of the diatom *T. weissflogii* and determine the effect of $p\text{CO}_2$ on the isotopic discrimination of Si (expressed as the enrichment factor ε). Silicic acid transport is cell cycle-dependent in diatoms with the greatest uptake rates during the G2 + M phase (Claquin et al. 2002). Because *T. weissflogii* cannot be synchronized, we grew cultures in continuous light in order to completely randomize (asynchronous growth) the cell cycle.

Methods and materials

Culture conditions—An axenic culture of the marine diatom *T. weissflogii* (clone Actin) was obtained from the Center for the Culture of Marine Protozoa. Continuous saturating irradiance was provided at a photon flux density of $160 \mu\text{mol m}^{-2} \text{s}^{-1}$ using fluorescent bulbs below the cultures. Temperature was maintained at 20°C . Cultures were grown using Aquil artificial seawater medium (Price et al. 1988/89), with some modifications. Macronutrients were added at $100 \mu\text{mol L}^{-1} \text{NO}_3^-$, $100 \mu\text{mol L}^{-1} \text{Si}(\text{OH})_4$ and $10 \mu\text{mol L}^{-1} \text{PO}_4^-$, and Zn was doubled ($\text{Zn}' = 30 \text{ pmol L}^{-1}$). Medium and culture flasks were microwave sterilized in polycarbonate (PC) bottles. All medium preparation and sample handling was carried out in a class 100 laminar flow hood. All plasticware was acid-cleaned by soaking in 10% trace metal grade HCl for 2–5 d and rinsed five times with $18.2 \text{ M}\Omega \text{ cm}$ deionized water. Unchelated (Zn' and Fe') metal concentrations were calculated using the thermodynamic equilibrium program Mineql (Westall et al. 1976). Axenicity was verified using acridine orange staining and epifluorescence microscopy.

High (750 ppm) and low (100 ppm) partial pressures of CO_2 were controlled using premixed gasses (Scott). Atmospheric level CO_2 was provided using laboratory air. Equilibrium was maintained by bubbling cultures with acid-washed plastic air diffusers, and, to ensure that partial pressures remained constant during growth, pH was monitored daily.

Growth and biomass measurements—Triplicate samples for cell counts and cell volume from each replicate flask were obtained using a Coulter particle counter (Model IIA) fitted with a $70\text{-}\mu\text{m}$ aperture. Growth was calculated from changes in cell counts through time. Cellular silicon quotas were obtained by filtering triplicate 20–40-ml aliquots of culture from each replicate flask onto $3.0\text{-}\mu\text{m}$ pore size PC (Poretics) filters. Total Si in biosilica was measured using $0.2 \text{ mol L}^{-1} \text{NaOH}$ digestion and colorimetric determination of Si (Paasche 1980).

Si uptake—Silicon uptake and efflux rates were obtained using ^{32}Si (Los Alamos Laboratory)–amended cultures. For long-term (1 h) uptake rates, cells were harvested at the mid-exponential phase ($[\text{Si}(\text{OH})_4]$ $40\text{--}50 \mu\text{mol L}^{-1}$) onto $3.0\text{-}\mu\text{m}$

pore size PC filters, rinsed, and resuspended in Si-free medium. Aliquots (25 ml) were dispensed into acid-cleaned duplicate PC tubes with Si additions of 0–25 $\mu\text{mol L}^{-1}$ and spiked with 315 Bq ^{32}Si . At the end of the incubation period, each tube was filtered onto 0.2- μm pore size 25-mm PC filters and rinsed with 3×10 ml radioisotope-free medium. The total amount of Si incorporated was determined by liquid scintillation counting and was calculated according to the method of Brzezinski and Phillips (1997). Uptake data were fitted to the Michaelis-Menten equation using nonlinear regression (Sigma plot 7.0).

Short-term (10 s) uptake rates were determined using a silicon oil centrifugation method (Badger et al. 1980; Tortell et al. 2000). Cells (2×10^7) were harvested at the mid-exponential phase ($[\text{Si}(\text{OH})_4]$ 40–50 $\mu\text{mol L}^{-1}$) onto 3.0- μm pore size PC filters, rinsed, and resuspended in 1 ml of bicine buffer with seawater salts (pH 8, $[\text{Si}(\text{OH})_4]$ = 50 $\mu\text{mol L}^{-1}$). Concentrated cells (200 μl) were layered on top of silicon oil in 0.6-ml microcentrifuge tubes. Illumination was provided from the side at a photon flux density of 500 $\mu\text{mol m}^{-2} \text{s}^{-1}$ using a tungsten-halogen bulb from a slide projector. To start the incubation, 315 Bq of ^{32}Si was added and mixed with the pipette. Incubations were terminated by centrifugation through the silicon oil layer into a basic terminating solution (2.5 mol L^{-1} NaOH and 10% methanol). The resulting pellet was immediately frozen in liquid nitrogen. The pellet was harvested by cutting off the base of the centrifuge tube and quantified using liquid scintillation counting, as described above.

Si efflux—Efflux rates were determined using 1-liter cultures grown at 100 and 750 ppm CO_2 in the presence of 12,600 Bq ^{32}Si for five to six generations. Efflux rates were determined by loading 2×10^6 cells, harvested at the mid-exponential phase ($[\text{Si}(\text{OH})_4]$ 40–50 $\mu\text{mol L}^{-1}$), onto an acid-cleaned 3- μm pore size, 25-mm PC filter supported on an acid-cleaned 25-mm PC cartridge (volume 1.6 ml). Illumination was provided from below at a photon flux density of 160 $\mu\text{mol m}^{-2} \text{s}^{-1}$ using fluorescent bulbs. At time zero, 15 ml of culture medium with a unlabeled silicic acid concentration of 100 $\mu\text{mol L}^{-1}$ was passed through the filter cartridge, to remove dissolved ^{32}Si label in bulk water and cell surface water, and discarded. At 2-min time intervals, a 5-ml volume of radioisotope-free medium was passed through the filter cartridge and collected for scintillation counting. The cartridge remained filled with seawater throughout the experiment, to avoid damage to the cells. Rinse medium was preequilibrated at 100 and 750 ppm $p\text{CO}_2$ and had a pH of 8.4 and 7.7, respectively. The calculated Si lost was fitted to raw and \log_{10} -transformed data using linear and nonlinear regression (Sigma lot 7.0), respectively.

Si dissolution—Si dissolution rates were measured according to the method of Bidle and Azam (2001). Axenic cultures (250 ml) were grown at 100 and 750 ppm CO_2 partial pressures in Aquil in the presence of 6,400 Bq ^{32}Si for six to seven generations. Triplicate samples (50 ml) were harvested in at the midexponential phase ($[\text{Si}(\text{OH})_4]$ 40–50 $\mu\text{mol L}^{-1}$). Cells were broken with seven rounds of freezing and thawing (-75 – 50°C) and incubated at 20°C and 100 and

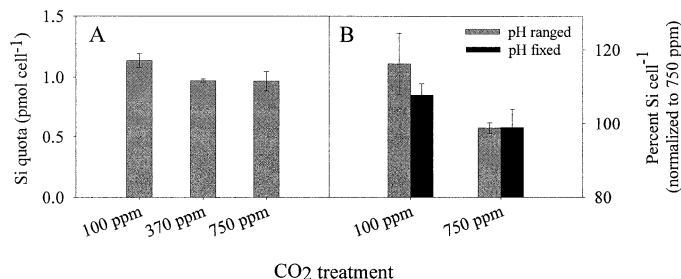


Fig. 2. Biogenic silica quotas as a function of $p\text{CO}_2$ in the diatom *T. weissflogii*. (A) Si quota. (B) Biogenic silica quotas as a percent of 750 ppm treatment. Comparison of fixed (8.3 ± 0.1) and ranging pH (100 ppm, pH = 8.5 ± 0.1 ; 750 ppm, pH = 7.8 ± 0.1). Error bars are 95% confidence intervals calculated from three replicates.

750 ppm CO_2 partial pressures for 48 h. Aliquots (5 ml) were filtered through 0.2- μm pore size sterile cartridge filters, and the filtrate was retained for scintillation counting. Specific and cell-normalized dissolution rates were calculated according to the method of Bidle and Azam (2001).

Effect of $p\text{CO}_2$ on diatom $\delta^{30}\text{Si}$ —Triplicate 2-liter cultures were grown under 100 and 750 ppm CO_2 partial pressures in Aquil with 200 $\mu\text{mol L}^{-1}$ silicic acid. After a 10% draw down of source silicic acid, the cultures were harvested by filtration onto 25-mm PC filters with 3- μm pore size. Dissolved-phase Si was collected from 0.2- μm PC filtrate. $\delta^{30}\text{Si}$ values for the dissolved $\text{Si}(\text{OH})_4$ and diatom silica (35 mmol Si per sample) were determined according to the method of De La Rocha et al. (1996).

Results

Si quota—Si quotas in *T. weissflogii* did not change with a rise of $p\text{CO}_2$ from 370 to 750 ppm, but a significant ($P < 0.001$, ANOVA) increase was observed at 100 ppm (Fig. 2A). To verify that the change in the Si quota was due to the partial pressure of CO_2 and not to pH-induced changes in metal speciation, control cultures were grown in which the pH was kept constant (pH 8.1 ± 0.5) over the CO_2 range by adjusting the carbonate alkalinity of the medium. Changes in the Si quota were found to be a function of CO_2 and not of pH (Fig. 2B). Growth rates were not significantly different across the range of $p\text{CO}_2$ treatments ($\mu = 1.4 \text{ d}^{-1} \pm 0.05$).

Si uptake in 1-h incubations—Si uptake rates as a function of external $\text{Si}(\text{OH})_4$ concentration did not show a detectable difference in the half-saturation constant (K_m) of high and low CO_2 -grown cells (Fig. 3). Increases in the maximum rate of uptake (V_{max}) of 25% were observed with increasing $p\text{CO}_2$, and these differences were greater (42%) when the data were normalized to Si quotas (specific rates).

Si influx and efflux—The unidirectional influx of Si was estimated using a 10-s uptake time course under the assumption of a negligible loss of ^{32}Si from the cell during that time. Over these short-term timescales (and saturating $\text{Si}(\text{OH})_4$ concentration of 50 $\mu\text{mol L}^{-1}$), there was no de-

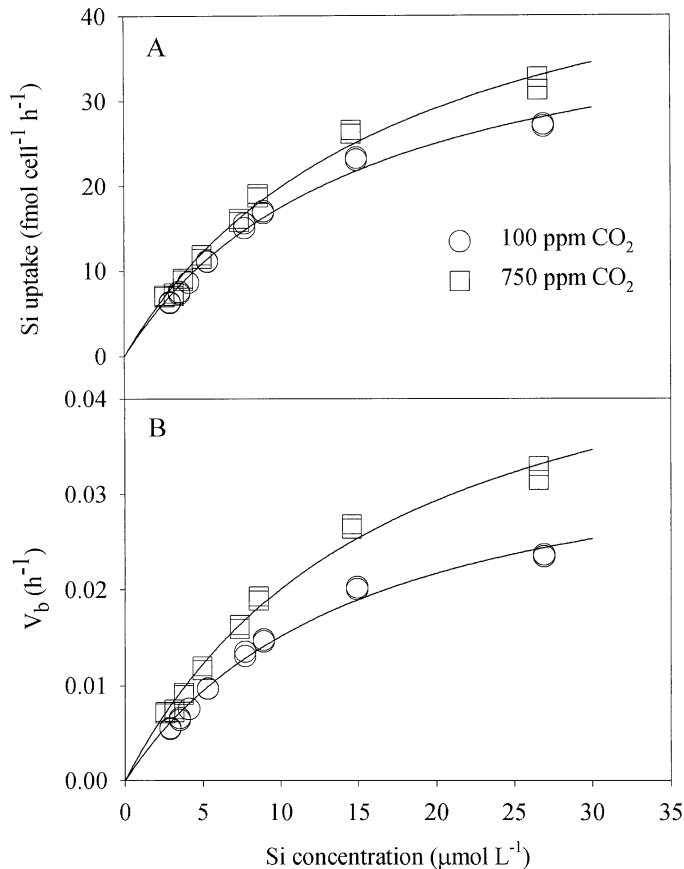


Fig. 3. *T. weissflogii* uptake kinetics of Si from 1-h incubations. (A) Cellular Si uptake rate. Michaelis-Menten fits, values, and SEs are 100 ppm: $k_m = 15.2 \pm 1.3$, $V_{max} = 44 \pm 2.1$; 750 ppm: $k_m = 17.4 \pm 1.5$, $V_{max} = 55 \pm 2.7$. (B) Specific Si uptake rate. 100 ppm: $k_m = 14.9 \pm 1.3$, $V_{max} = 0.038 \pm 0.002$; 750 ppm: $k_m = 17 \pm 1.4$, $V_{max} = 0.054 \pm 0.003$. Raw data from two replicates.

tectable difference in influx between low and high CO₂ (Fig. 4). The rates obtained were twofold higher than those under saturating conditions (50 $\mu\text{mol L}^{-1}$ Si(OH)₄) using incubations of 1 h (Fig. 3). Unidirectional efflux rates of ³²Si were determined under steady state, saturating Si(OH)₄ concentrations (100 $\mu\text{mol L}^{-1}$) and with the assumption of no recapture of ³²Si after efflux. The efflux of Si was greater at 750 ppm than at 100 ppm CO₂ (Fig. 5). Losses of ³²Si from both high and low CO₂ showed a two-phase kinetic system. Each kinetic phase represents an internal cellular compartment of Si, with characteristic fluxes (fmol Si cell⁻¹ min⁻¹) and exchange constants (k_a , k_b min⁻¹) given as the y intercept and slope, respectively (Fig. 5B) (MacRobbie 1971). Although it is not possible to identify the intracellular location of each pool with these data alone, the turnover times ($\ln 2/k_a \sim 7$ min $\ln 2/k_b \sim 50$ min) are on the order of turnover times for nitrogen in vascular plant cytosol (10 min) and vacuoles (100 min) (Britto and Kronzucker 2001; Britto et al. 2001).

Si dissolution—Silica dissolution rates of freeze-thaw-prepared, axenic frustules were dependent on ambient CO₂ (Fig. 6). At low CO₂, the specific dissolution (V_{diss}) was 0.6% d⁻¹ or 8 fmol cell⁻¹ d⁻¹. Incubations under high CO₂ resulted

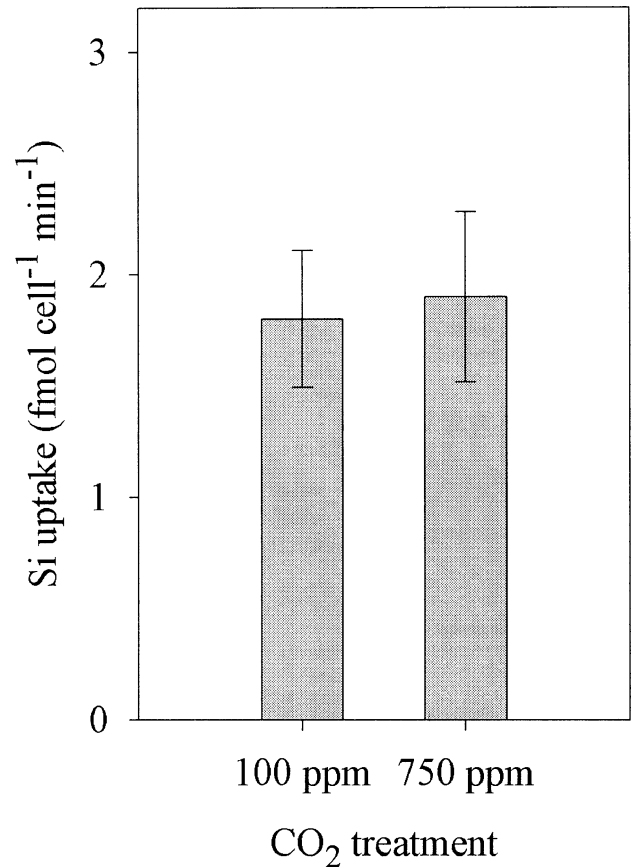


Fig. 4. Short-term (10 s) unidirectional influx rates at high and low $p\text{CO}_2$ from the silicon oil centrifugation technique. Error bars are 95% confidence intervals, calculated from three replicates.

in a six- to sevenfold increase in dissolution rates ($V_{diss} = 4\% \text{ d}^{-1}$ or 40 fmol⁻¹ cell d⁻¹).

Si isotope discrimination—In incubations for silicon isotope measurements, the Si(OH)₄ concentration was drawn down 10–15% (Table 1). At this low substrate utilization, we assumed that the difference between the substrate [Si(OH)₄] and product (silica) was equivalent to the enrichment factor ϵ ($\epsilon = {}^{30}\delta\text{Si Si(OH)}_4 - {}^{30}\delta\text{Si silica}$). The enrichment factor was not affected by $p\text{CO}_2$ in *T. weissflogii* (Table 1). The average value of ϵ , -1.5‰ was somewhat higher than the value of -1.1‰ determined for this species by De La Rocha et al. (1997) but was within the reported error of the method.

Discussion

Cellular mass-balance model of Si—The results of Si quota and flux measurements can be used to formulate a Si mass-balance model for asynchronous *T. weissflogii* growing under saturating silicic acid concentrations ($[\text{Si(OH)}_4] \geq 40 \mu\text{mol L}^{-1}$) at high and low $p\text{CO}_2$ (Fig. 7). In this calculation, we pooled the two-compartment efflux (Fig. 5B) into a single flux, to avoid making assumptions of how the internal pools are connected. The averages of our independent flux

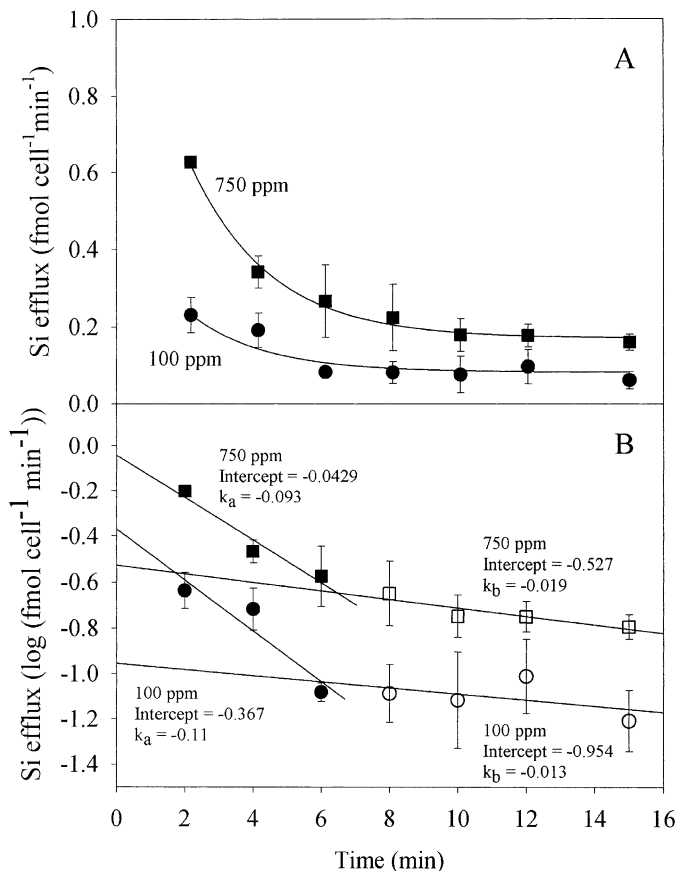


Fig. 5. (A) ³²Si efflux curves for fully labeled (8–10 generations) *T. weissflogii* grown at high and low *p*CO₂. (B) Log (base 10) transformed efflux curves showing the linear regressions of each efflux phase. Error bars are 95% confidence intervals, calculated from three replicates.

measurements nearly satisfy the mass balance condition: influx = incorporation + efflux + dissolution, particularly in the cells grown under high *p*CO₂. An exact mass balance can be obtained within the precision of the data, bolstering our confidence in the methodology. The influx rates of Si were nearly equal at the two *p*CO₂ treatments, but the rates of dissolution, efflux, and incorporation into the frustule differed. When grown under low *p*CO₂, *T. weissflogii* retained the Si taken up with greater efficiency than when grown under high *p*CO₂.

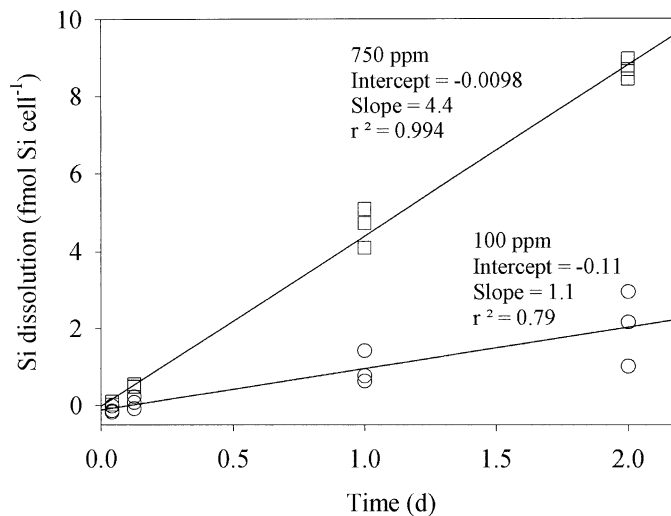


Fig. 6. Dissolution of Si in broken, axenic frustules as a function of time in high and low *p*CO₂. Raw data from three replicates.

Efflux and dissolution—Laboratory studies have shown that, in the absence of bacteria, there is very little dissolution (0.4–0.9% d⁻¹) of silica from diatom detritus that retains the organic covering over the frustule (Bidle and Azam 2001). Our results for axenic dissolution rates agree well with those of Bidle and Azam (2001) but only under low CO₂. At high CO₂, we were surprised to find that dissolution rates were six- to sevenfold higher and that the highest dissolution rate was observed at low pH (7.7) rather than at high pH (8.4), as expected for SiO₂. We were able to rule out bacterially enhanced dissolution and to foresee three possibilities for this response. (1) Frustules produced under high CO₂ growth conditions may differ in the degree to which organic matter is effective in protecting silica from dissolution. (2) A decrease in the Si quota results in a change in the architecture of the frustule and a higher surface area of silica. A high surface area has been shown to be correlated with high dissolution rates (Dixit et al. 2001). (3) The increase in dissolution is an indirect effect of the decrease in pH. At pH 7.8, 20% of the aluminum (present as a trace contaminant in the medium) was chelated by EDTA, whereas aluminum was unchelated at pH 8.4 and was more bioavailable. The incorporation of unchelated aluminum in the silica matrix could decrease silica dissolution rates (Van Cappellen et al. 2002). Further work is needed to determine the degree to which any of these factors drive dissolution rates.

Table 1. Isotopic discrimination of frustule Si (³⁰Si: ²⁸Si) in *T. weissflogii* grown under high and low *p*CO₂.

<i>p</i> CO ₂ treatment (%)	Si(OH) ₄ drawdown (μmol L ⁻¹)	Si(OH) ₄ drawdown (%)	Soluble phase δ ³⁰ Si (‰)	Particulate phase δ ³⁰ Si (‰)	Isotope effect ε ³⁰ Si (‰)
100	26.8	13.1	0.124	-1.43	-1.55
	30.2	14.6	0.083	-1.45	-1.53
	23.6	11.6	NA	-1.25	
750	19.9	10.1	0.141	-1.41	-1.56
	21.5	10.9	0.114	-1.63	-1.75
	19.5	9.8	0.079	-1.43	-1.51

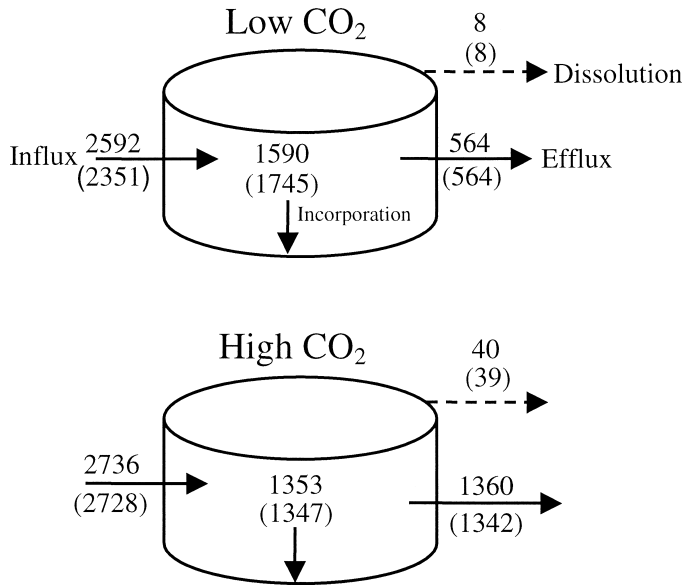


Fig. 7. Mass balanced flux model in units of fmol Si cell⁻¹ d⁻¹ for *T. weissflogii* grown under low and high pCO₂. Cylinders represent the silica cell wall (frustule). Influx, efflux, and dissolution are measured. Incorporation into frustule is calculated as Si quota × growth rate ($\mu = 1.4\text{ d}^{-1}$). Fluxes are mean values. Mass-balanced values, in parentheses, were calculated using Microsoft Excel solver to iteratively solve for $0 = \text{influx} - \text{efflux} - \text{dissolution} - \text{incorporation}$. The iteration was constrained to 6% variation around each mean flux value.

Measurements of Si dissolution rates using ²⁹Si isotope dilution are affected by Si efflux. In such studies, a highly enriched heavy isotope of silicon is added to an incubation, and, because there are insignificant differences between ²⁸Si and ²⁹Si incorporation rates, the dilution of the heavy isotope pool established by adding ²⁹Si to the seawater results from the dissolution of relatively light silica. However, the exchange of internal pools of Si(OH)₄ early in the experiment, before the isotopic composition of the cellular pools have equilibrated with the Si(OH)₄ in the seawater, results in further isotopic dilution and an overestimation of dissolution. The extent of this overestimate is a function of incubation time and can be calculated on the basis of the data in Fig. 5. On the basis of these calculations (Fig. 8), we can reconcile the relatively high dissolution rates obtained in culture by Nelson et al. (1976) and in the field (Brzezinski et al. 2003) with the low rates reported by Bidle and Azam (2001) and confirmed in the present study (Fig. 6). Nelson et al. (1976) measured apparent specific dissolution rates (V_{diss}) of 5–20% d⁻¹ in 4-h incubations. This is in accord with our prediction that the efflux rates from *T. weissflogii* should give apparent dissolution rates of 6–18% d⁻¹ in 4-h incubations (Fig. 8).

During diatom bloom events, Brzezinski et al. (2003) measured apparent dissolution rates of ~5% of silica production on the basis of 24-h incubations. This is of the same order of magnitude as the ratio of our efflux rates to Si transport (3–5%) for the contribution of efflux of intracellular Si to dissolution: production rate ratios measured using isotope dilution. This comparison suggests that the low rates

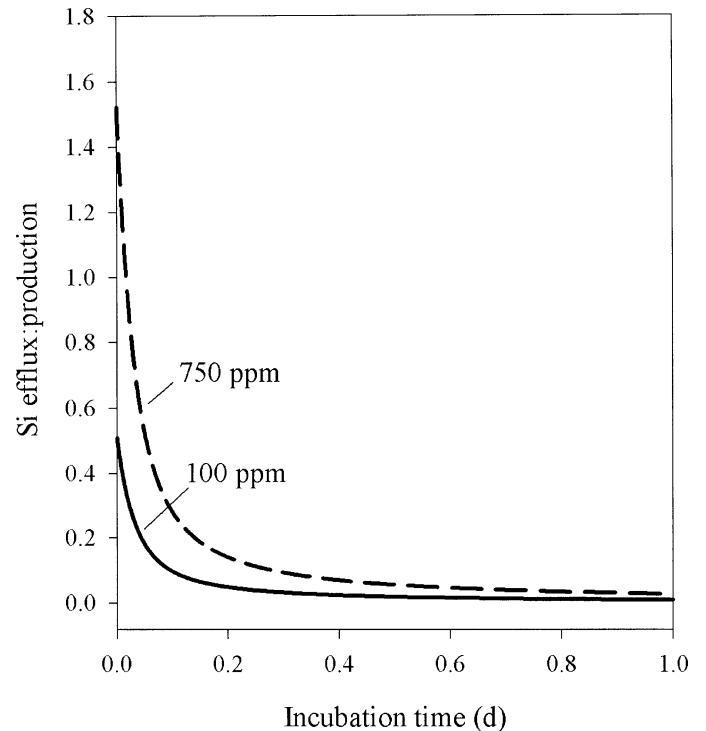
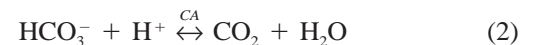


Fig. 8. The apparent Si dissolution rate calculated from efflux. Efflux: production rates versus incubation time are calculated E:P was calculated using fluxes from Fig. 7, under the assumption of an internal pool of 50 fmol cell⁻¹ and isotope ratios (²⁸Si:(²⁸Si + ²⁹Si + ³⁰Si)) of 50% for internal and 92% for external. Curves follow the form $E:P_{750} = 1.24 \times e^{(-k_a t)} + 0.23 \times e^{(-k_b t)}$, $E:P_{100} = 0.42 \times e^{(-k_a t)} + 0.08 \times e^{(-k_b t)}$ where $k_a = 26\text{ d}^{-1}$ and $k_b = 2.6\text{ d}^{-1}$.

of dissolution measured during blooms may represent the efflux of internal dissolved pools rather than the true dissolution of frustules. It is possible that the frustules of living diatoms do not dissolve at ecologically significant rates. This is advantageous for diatoms, because daughter cells inherit half of their frustule from the mother cell, and there is no known repair mechanism for diatom silica after its deposition. The dissolution of otherwise healthy diatoms would mean that the quality of the inherited frustule would decline with each generation, with likely detrimental effects once the structural integrity of the structure is compromised. During postbloom conditions, measured rates of silica dissolution are sufficiently high (60–80%) that efflux from live cells would have little effect on the calculated rates.

CO₂ effects on Si quota—Diatoms possess a carbon concentrating mechanism that uses an extracellular carbonic anhydrase (CA) and catalyses the following equilibrium reaction (Burkhardt et al. 2001; Morel et al. 2002).



Catalysis allows maintenance of the equilibrium concentration of CO₂ (10 μmol L⁻¹, given an seawater alkalinity of 2.3 mmol L⁻¹ and 20°C) at the surface of the cell, and permits access to the high concentrations of bicarbonate (~2 mmol L⁻¹) in seawater. Forms of CA that have high catalytic

rates ($K_{\text{cat}} > 10^3 \text{ s}^{-1}$) require a pH buffer to either provide or receive the proton in the above reaction, because proton exchange with water is relatively slow compared with the rate of catalysis. The silica frustule has been shown to be an effective pH buffer for the CA-mediated conversion of bicarbonate to CO_2 , and the activity of external CA increases dramatically in *T. weissflogii* grown at 100 ppm CO_2 (Milligan and Morel 2001). The increase in Si quota at low $p\text{CO}_2$, which is concomitant with an increase in CA activity, is consistent with its role as a buffer for CA.

It has been demonstrated that both iron and zinc play a role in modifying the Si:N relationship in diatoms (Rueter and Morel 1981; Hutchins and Bruland 1998; De La Rocha et al. 2000). Iron limitation increases the Si:N ratio in cultured phytoplankton by two- to threefold and Si:N uptake ratios in field populations of Antarctic diatoms from 2–8 (Franck et al. 2000). Zinc limited growth of cultured diatoms results in a decrease in Si:N ratio (De La Rocha et al. 2000). It is unlikely that the Si quota changes we measured resulted from changes in the trace metal availability. Both iron and zinc were provided at saturating concentrations (100 ppm: $\text{Fe}' = 133 \text{ nmol L}^{-1}$, $\text{Zn}' = 16 \text{ pmol L}^{-1}$; 750 ppm: $\text{Fe}' = 10 \text{ nmol L}^{-1}$, $\text{Zn}' = 12 \text{ pmol L}^{-1}$), and the Si quota changed with $p\text{CO}_2$ whether pH varied or was kept constant by varying carbonate alkalinity.

Several researchers have hypothesized that the growth rate limitation of diatoms by nutrients other than Si results in increases in the Si:N ratio (Flynn and Martin-Jézéquel 2000; Claquin et al. 2002). The ability of *T. weissflogii* to control Si quota through efflux of Si suggests that quota changes are not simply a function of cell cycle, as was suggested by Claquin et al. (2001). Those authors reasoned that, because the major transport of Si is during the G2 + M phase of the cell cycle, a change in the Si quota may be driven by the length of time a cell spends in these phases. In the present study, changes in the Si quota with $p\text{CO}_2$ are not accompanied by a concomitant change in growth rate. This is consistent with an efficient carbon-concentrating mechanism and with observations in field incubations of natural diatom assemblages that show little change in growth rate over a large CO_2 range (Tortell et al. 1997, 2000). Changes in the Si efflux presumably reflect the fine control of silicon metabolism by diatoms. It is possible for the duration of a particular cell=cycle stage to change without a change in the duration of the total cell cycle, although the G2 + M phase of the cell cycle is the least variable in duration (Guiget et al. 1984). If this were the case, the expression of Si transporters during G2 + M could occur over a longer time period at low CO_2 . However, our results indicate that the Si efflux is regulated and that this regulation is not necessarily a function of Si transporter expression. The diffusion of Si species (either uncharged Si(OH)_4 or organically bound forms of Si(OH)_4) across the cell membrane is a possible means of exit from the cell. We propose that there are additional controls on Si quota that were not envisioned in the Claquin et al. (2002) model. The mechanisms by which Si is regulated in diatoms remains unclear, and elucidation awaits molecular-level studies of the regulatory steps involved.

Silicon isotopes—Silicon isotope fractionation has been measured in three species of diatoms grown under three temperatures and the fractionation factor ($\epsilon = -1.1\% \pm 0.4$) was found to be similar, regardless of species tested or their rates of growth (De La Rocha et al. 1997). It has been suggested that the most likely explanation for a consistent fractionation factor is that the transport of Si across the membrane is the discriminatory step in the biomineralization process. Alternatively, a step internal to the cell (i.e., polymerization) could be the site of discrimination. The variation in the efflux:influx ratio caused by $p\text{CO}_2$ is an ideal tool to test these opposing explanations.

If the isotope discrimination is intracellular, the isotopic effect can be scaled linearly to the efflux:influx ratio (Eq. 1; Popp et al. 1989). We would then expect low $p\text{CO}_2$ grown cells to have a 2.3-fold lower $\delta^{30}\text{Si}$ signal than high CO_2 cells (Fig. 7). The lack of difference in the $\delta^{30}\text{Si}$ signal under low and high $p\text{CO}_2$ supports the notion that Si discrimination occurs at the membrane transport step and that the loss of Si from the cell has no measurable isotope effect (i.e., $\epsilon_{i2} \sim 0$). The fact that the isotope effect for Si is small (1.5%) may also be evidence of discrimination at the level of transport, which may not necessitate breaking or forming chemical bonds. Of importance, this finding supports the use of the silica $\delta^{30}\text{Si}$ signal as an indicator of the extent of Si(OH)_4 utilization in surface waters both in paleo- and contemporary studies, because diatom physiology is unlikely to affect the $\delta^{30}\text{Si}$ value of the frustule.

Oceanographic implications—The increase in the Si quota at low $p\text{CO}_2$ may increase diatom Si:C and, hence, reduce the flux of diatom carbon export to deep waters for a given level of silica production. High $p\text{CO}_2$ would favor lower diatom Si:C ratios, potentially increasing diatom C flux; however, this effect would be partially offset by the higher rates of silica dissolution under high $p\text{CO}_2$. These effects act in concert with other factors such as the influence of bacteria on silica dissolution (Bidle and Azam 2001). Bacterially mediated silica dissolution is likely to be a more important control on the coupling between diatom Si and C cycling than is $p\text{CO}_2$ (Bidle and Azam 2001; Brzezinski et al. 2003). The $p\text{CO}_2$ -induced changes in Si quotas of *T. weissflogii* are small ($\sim 20\%$), but further work on other diatoms, particularly heavily silicified Antarctic species, is required to determine the range of possible impacts of $p\text{CO}_2$ on Si quotas.

References

- BADGER, M. R., A. KAPLAN, AND J. A. BERRY. 1980. Internal inorganic carbon pool of *Chlamydomonas reinhardtii*—evidence for a carbon-dioxide concentrating mechanism. *Plant Physiol.* **66**: 407–413.
- BIDLE, K. D., AND F. AZAM. 2001. Bacterial control of silicon regeneration from diatom detritus: Significance of bacterial ecto-hydrolases and species identity. *Limnol. Oceanogr.* **46**: 1606–1623.
- BRITTO, D. T., AND H. J. KRONZUCKER. 2001. Can unidirectional influx be measured in higher plants? A mathematical approach using parameters from efflux analysis. *New Phytol.* **150**: 37–47.
- , M. Y. SIDDIQI, A. D. M. GLASS, AND H. J. KRONZUCKER.

2001. Futile transmembrane NH₄⁺ cycling: A cellular hypothesis to explain ammonium toxicity in plants. *Proc. Natl. Acad. Sci. USA* **98**: 4255–4258.
- BRZEZINSKI, M. A., J. L. JONES, K. D. BIDLE, AND F. AZAM. 2003. The balance between silica production and silica dissolution in the sea: Insights from Monterey Bay California applied to the global data set. *Limnol. Oceanogr.* **48**: 1846–1854.
- , AND D. R. PHILIPS. 1997. Evaluation of ³²Si as a tracer for measuring silica production rates in marine waters. *Limnol. Oceanogr.* **42**: 856–865.
- , AND OTHERS. 2002. A switch from Si(OH)₄ to NO₃⁻ depletion in the glacial Southern Ocean. *Geophys. Res. Lett.* **29**: 1564.
- BURKHARDT, S., G. AMOROSO, U. RIEBESELL, AND D. SÜLTEMEYER. 2001. CO₂ and HCO₃⁻ uptake in marine diatoms acclimated to different CO₂ concentrations. *Limnol. Oceanogr.* **46**: 1378–1391.
- CLAQUIN, P., V. MARTIN-JÉZÉQUEL, J. C. KROMKAMP, M. J. W. VELDUIS, AND G. KRAY. 2002. Uncoupling of silicon compared to carbon and nitrogen metabolisms, and the role of the cell cycle, in continuous cultures of *Thalassiosira pseudonana* (Bacillariophyceae) under light, nitrogen and phosphorus control. *J. Phycol.* **38**: 922–930.
- DE LA ROCHA, C. L., M. A. BRZEZINSKI, AND M. J. DENIRO. 1996. Purification, recovery, and laser-driven fluorination of silicon from dissolved and particulate silica for the measurement of natural stable isotope abundances. *Analyt. Chem.* **68**: 3746–3750.
- , ———, AND ———. 1997. Fractionation of silicon isotopes by marine diatoms during biogenic silica formation. *Geochim. Cosmochim. Acta* **61**: 5051–5056.
- , ———, ———, AND A. SHEMESH. 1998. Silicon-isotope composition of diatoms as an indicator of past oceanic change. *Nature* **395**: 680–683.
- , D. A. HUTCHINS, M. A. BRZEZINSKI, AND Y. H. ZHANG. 2000. Effects of iron and zinc deficiency on elemental composition and silica production by diatoms. *Mar. Ecol. Prog. Ser.* **195**: 71–79.
- DIXIT, S., P. VAN CAPPELLEN, AND A. J. VAN BENNEKOM. 2001. Processes controlling solubility of biogenic silica and pore water build-up of silicic acid in marine sediments. *Mar. Chem.* **73**: 333–352.
- DUGDALE, R. C., AND F. P. WILKERSON. 1998. Silicate regulation of new production in the equatorial Pacific upwelling. *Nature* **391**: 270–273.
- FLYNN, K. J., AND V. MARTIN-JÉZÉQUEL. 2000. Modeling Si-N-limited growth of diatoms. *J. Plankton Res.* **22**: 447–472.
- FRANCK, V. M., M. A. BRZEZINSKI, K. H. COALE, AND D. M. NELSON. 2000. Iron and silicic acid concentrations regulate Si uptake north and south of the Polar Frontal Zone in the Pacific Sector of the Southern Ocean. *Deep-Sea Res.* **47**: 3315–3338.
- GUIGET, M., J.-J. KUPIEC, AND A.-J. VALLERON. 1984. A systematic study of the variability of the cell cycle phase durations in experimental mammalian systems, pp. 97–111. *In* L. N. Edmunds Jr. [ed.], *Cell cycle clocks*. Marcell Dekker.
- HUTCHINS, D. A., AND K. W. BRULAND. 1998. Iron-limited diatom growth and Si:N uptake ratios in a coastal upwelling regime. *Nature* **393**: 561–564.
- MACROBBIE, E. A. C. 1971. Fluxes and compartmentation in plant cells. *Annu. Rev. Plant Physiol.* **42**: 335–353.
- MILLIGAN, A. J., AND F. M. M. MOREL. 2002. A proton buffering role for silica in diatoms. *Science* **297**: 1848–50.
- MOREL, F. M. M., AND OTHERS. 2002. Acquisition of inorganic carbon by the marine diatom *Thalassiosira weissflogii*. *Funct. Plant Biol.* **29**: 301–308.
- NELSON, D. M., J. J. GOERING, S. S. KILHAM, AND R. R. L. GUIL-LARD. 1976. Kinetics of silicic-acid uptake and rates of silica dissolution in marine diatom *Thalassiosira-pseudonana*. *J. Phycol.* **12**: 246–252.
- PAASCHE, E. 1980. Silicon content of five marine plankton diatom species measured with a rapid filter method. *Limnol. Oceanogr.* **25**: 474–480.
- POPP, B. N., R. TAKIGIKU, J. M. HAYES, J. W. LOUDA, AND E. W. BAKER. 1989. The post-paleozoic chronology and mechanism of ¹³C depletion in primary marine organic matter. *Am. J. Sci.* **289**: 436–454.
- PRICE, N. M., G. I. HARRISON, J. G. HERING, R. J. HUDSON, P. M. V. NIREL, B. PALENIK, AND F. M. M. MOREL. 1988/89. Preparation and chemistry of the artificial algal culture medium Aquil. *Biol. Oceanogr.* **6**: 443–61.
- RAGUENEAU, O., AND OTHERS. 2000. A review of the Si cycle in the modern ocean: recent progress and missing gaps in the application of biogenic opal as a paleoproductivity proxy. *Global Planet. Change* **26**: 317–365.
- RUETER, J. G., AND F. M. M. MOREL. 1981. The interaction between zinc-deficiency and copper toxicity as it affects the silicic-acid uptake mechanisms in *Thalassiosira pseudonana*. *Limnol. Oceanogr.* **26**: 67–73.
- SULLIVAN, C. W. 1976. Diatom mineralization of silicic acid. I. Si(OH)₄ transport characteristics in *Navicula pelliculosa*. *J. Phycol.* **12**: 390–396.
- TORTELL, P. D., G. H. RAU, AND F. M. M. MOREL. 2000. Inorganic carbon acquisition in coastal Pacific phytoplankton communities. *Limnol. Oceanogr.* **45**: 1485–1500.
- , J. R. REINFELDER, AND F. M. M. MOREL. 1997. Active bicarbonate uptake by diatoms. *Nature* **390**: 243–244.
- WESTALL, J. C., J. L. ZACHARY, AND F. M. M. MOREL. 1976. Mineql, a computer program for the calculation of chemical equilibrium composition of aqueous systems. *Civil Engineer. Mass. Inst. Tech.*

Received: 21 April 2003

Accepted: 16 September 2003

Amended: 8 October 2003